



CERN-EP-2016-018
26 January 2016

Anisotropic flow of charged particles in Pb–Pb collisions at $\sqrt{s_{NN}}=5.02$ TeV

ALICE Collaboration*

Abstract

We report the first results of elliptic (v_2), triangular (v_3) and quadrangular flow (v_4) of charged particles in Pb–Pb collisions at a center-of-mass energy per nucleon pair of $\sqrt{s_{NN}} = 5.02$ TeV with the ALICE detector at the CERN Large Hadron Collider. The measurements are performed in the central pseudorapidity region $|\eta| < 0.8$ and for the transverse momentum range $0.2 < p_T < 5$ GeV/c. The anisotropic flow is measured using two-particle correlations with a pseudorapidity gap greater than one unit and with the multi-particle cumulant method. Compared to results from Pb–Pb collisions at $\sqrt{s_{NN}} = 2.76$ TeV, the anisotropic flow coefficients v_2 , v_3 and v_4 are found to increase by $(3.0 \pm 0.6)\%$, $(4.3 \pm 1.4)\%$ and $(10.2 \pm 3.8)\%$, respectively, in the centrality range 0–50%. This increase can be attributed mostly to an increase of the average transverse momentum between the two energies. The measurements are found to be compatible with hydrodynamic model calculations. This comparison provides a unique opportunity to test the validity of the hydrodynamic picture and the power to further discriminate between various possibilities for the temperature dependence of shear viscosity to entropy density ratio of the produced matter in heavy-ion collisions at the highest energies.

arXiv:1602.01119v2 [nucl-ex] 4 Apr 2016

© 2016 CERN for the benefit of the ALICE Collaboration.

Reproduction of this article or parts of it is allowed as specified in the CC-BY-4.0 license.

*See Appendix A for the list of collaboration members

The goal of studies with relativistic heavy-ion collisions is to investigate the Quark-Gluon Plasma (QGP), a state of matter where quarks and gluons move freely over distances large in comparison to the typical size of a hadron. The transition from normal nuclear matter to the QGP state is expected to occur at extreme values of energy density (0.2–0.5 GeV/fm³, according to lattice Quantum Chromodynamics calculations [1, 2]), which are accessible in ultra-relativistic heavy-ion collisions at the Large Hadron Collider (LHC) [3, 4]. The study of such collisions provides the unique opportunity to probe the properties of the QGP in a region of the QCD phase diagram where a cross-over between the deconfined phase and normal nuclear matter is expected [5–9].

Studies of the azimuthal anisotropy of particle production have contributed significantly to the characterization of the system created in heavy-ion collisions [10, 11]. Anisotropic flow, which measures the momentum anisotropy of the final-state particles, is sensitive both to the initial geometry of the overlap region and to the transport properties and equation of state of the system. By using a general Fourier series decomposition of the azimuthal distribution of produced particles:

$$\frac{dN}{d\varphi} \propto 1 + 2 \sum_{n=1}^{\infty} v_n \cos[n(\varphi - \Psi_n)], \quad (1)$$

anisotropic flow is quantified with coefficients v_n and corresponding symmetry planes Ψ_n [12]. Due to the approximately ellipsoidal shape of the overlap region in non-central heavy-ion collisions (i.e. collisions that correspond to large impact parameter), the dominant flow coefficient is v_2 , referred to as elliptic flow. In the transition from highest RHIC to LHC energies, elliptic flow increases by 30% [13], as predicted by hydrodynamic models that include viscous corrections [14–18]. Non-vanishing values of higher anisotropic flow harmonics v_3 – v_6 at the LHC are ascribed primarily to the response of the produced QGP to fluctuations of the initial energy density profile of the colliding nucleons [19–22]. Moreover, due to such fluctuations each flow harmonic v_n has a distinct symmetry plane Ψ_n and recent measurements of their inter-correlations provide independent constraints on the QGP properties [23]. The combination of all of such results demonstrates that the shear viscosity to entropy density ratio (η/s) of the QGP produced in ultra-relativistic heavy-ion collisions at RHIC and LHC has a value close to $1/4\pi$, a lower bound obtained in strong-coupling calculations based on the AdS/CFT conjecture [24].

Recently, predictions from Niemi et al. on anisotropic flow coefficients for Pb–Pb $\sqrt{s_{\text{NN}}} = 5.02$ TeV collisions using the EKRT model were reported in [25]. These predictions have a special emphasis on the discriminating power between various parameterizations of the temperature dependence of η/s . It was argued that in the transition from 2.76 to 5.02 TeV, the elliptic flow estimated from two-particle correlations (denoted further in the text as $v_2\{2\}$, where the number in the curly brackets indicates the number of particles that are used in correlation [26]) can increase at most $\sim 5\%$ for all centrality classes. Details of the increase depend on the parameterization of $\eta/s(T)$. On the other hand, higher flow harmonic observables, like $v_3\{2\}$ and $v_4\{2\}$, are predicted to increase more rapidly, 10 – 30%. With a different approach, where previously measured values of flow harmonics at lower LHC energies are taken as a baseline, Noronha-Hostler et al. [27] predict a larger increase for both elliptic and triangular flow in peripheral compared to central collisions in transition from 2.76 to 5.02 TeV. They conclude that the anisotropic flow already reaches saturation and its maximum value in central collisions at 2.76 TeV.

A necessary condition for the development of anisotropic flow is the initial anisotropy in the interaction region of the two colliding ions. These coordinate space anisotropies are described in terms of eccentricities, that are not directly accessible experimentally. Nonetheless, the theoretical modeling of such eccentricities is actively being studied. For instance, hydrodynamic calculations based on a MC-Glauber model and MC-KLN initial conditions do not agree on the details of the saturation of elliptic flow at LHC energies [28]. However, with these two initial state models, it was shown that the final spatial eccentricity decreases monotonically as the collision energy increases [28], and is expected to become negative only at the very large collision energies available at the LHC (see Fig. 9 in [28]).

In addition to the initial conditions, various other stages of evolution of the system in a heavy-ion collision may contribute to the development of anisotropic flow. At lower energies, the state of the system will resemble primarily a hadronic gas, and hadron rescattering is the dominant contribution to the anisotropic flow. At higher energies, anisotropic flow mostly develops in the thermalized color-deconfined QGP phase. However, even at these higher energies, the contribution from the hadronic phase can be significant. The relative amount of time the system spends in different phases varies with collision energy [28, 29]. Radial flow, a measure for the average velocity of the system's collective radial expansion, also increases as a function of collision energy, which translates into more particles being transferred to a higher transverse momentum (p_T) region, thus leading to an increase in average anisotropic flow values. On the other hand, the opposite dependence of differential $v_2(p_T)$ is expected for light (increase at low p_T) and heavy particles (decrease at low p_T) as a function of collision energy, which might yield to the saturation of elliptic flow signal [28]. Finally, the relative importance of various stages in the system evolution as a function of collision energy can also vary for each flow coefficient [29].

The data used in this Letter were recorded with the ALICE detector [30, 31] in November 2015 in Run 2 at the LHC with Pb–Pb collisions at $\sqrt{s_{NN}} = 5.02$ TeV. Minimum bias Pb–Pb events were triggered by the coincidence of signals from the V0 detector. The V0 detector is composed of two arrays of scintillator counters, V0-A and V0-C, which cover the pseudorapidity ranges $2.8 < \eta < 5.1$ and $-3.7 < \eta < -1.7$, respectively [30]. Centrality quantifies the fraction of geometrical cross-section of the colliding nuclei. It is determined using the sum of the amplitudes of the V0-A and C signals, which provides a resolution better than 0.5% up to 20% central Pb–Pb collisions, and better than 2% for peripheral collisions [32]. The offline event selection employs the information from two Zero Degree Calorimeters (ZDC) [30] positioned 112.5 m from the interaction point on either side. Beam background events are removed using timing information from the V0 and the ZDC, respectively. To ensure a uniform acceptance and reconstruction efficiency in the pseudorapidity region $|\eta| < 0.8$, only events with a reconstructed vertex within 10 cm from the center of the detector along the beam direction were used. A sample of 140 k PbPb collisions events passed the selection criteria. Only one low luminosity run (with trigger rate of 27 Hz) was used, being least affected by pile-up and distortions from space charge in the main tracking detector, the Time Projection Chamber (TPC).

Charged tracks are reconstructed using the ALICE Inner Tracking System (ITS) and TPC [30]. This combination ensures a high detection efficiency, optimum momentum resolution, and a minimum contribution from photon conversions and secondary charged particles produced either from the detector material or from weak decays. In order to reduce the contamination from secondary particles, only tracks with a distance of closest approach (DCA) to the interaction point of less than 3 cm, both in the longitudinal and transverse directions, are accepted. The tracking efficiency is calculated from a Monte Carlo simulation that uses HIJING [33] to simulate particle production. GEANT3 [34] is then used for transporting simulated particles, followed by a full calculation of the detector response (including production of secondary particles) and track reconstruction performed with the ALICE reconstruction framework. The tracking efficiency is $\sim 70\%$ at $p_T \sim 0.2$ GeV/ c and increases to an approximately constant value of $\sim 80\%$ for $p_T > 1$ GeV/ c . The p_T resolution is better than 5% for the region presented in this Letter. The systematic uncertainty related to the non-uniform reconstruction efficiency was found to be at the level of 1%. The flow coefficients from tracks that are reconstructed from TPC space points alone were compared to coefficients extracted from particles that used both TPC clusters and ITS hits, which were found to agree within $\sim 2\%$. This difference was taken into account in the estimation of the systematic uncertainty. Altering the selection criteria for the tracks reconstructed with the TPC resulted in a variation of the results of 0.5%, at most. Other selection criteria that have been scrutinized are the centrality determination, e.g. using the Silicon Pixel Detector (SPD), which contributed by less than 1%, the polarity of the magnetic field of the ALICE detector and the position of the reconstructed primary vertex, whose contributions were found to be negligible. The systematic uncertainties evaluated for each of the sources mentioned above were added in quadrature to obtain the total systematic uncertainty of

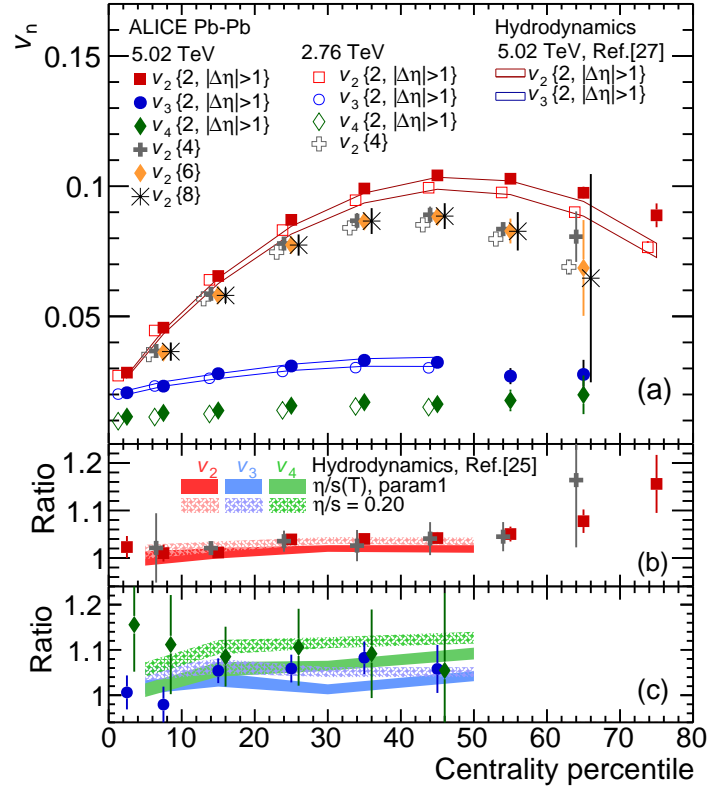


Fig. 1: (color online) (a) Anisotropic flow v_n integrated over the p_T range $0.2 < p_T < 5.0$ GeV/ c , as a function of event centrality, for the two-particle (with $|\Delta\eta| > 1$) and multi-particle cumulant methods. Measurements for Pb–Pb collisions at $\sqrt{s_{NN}} = 5.02$ (2.76) TeV are shown by solid (open) markers [20]. The ratios of $v_2\{2, |\Delta\eta| > 1\}$ (red), $v_2\{4\}$ (gray) and $v_3\{2, |\Delta\eta| > 1\}$ (blue), $v_4\{2, |\Delta\eta| > 1\}$ (green) between Pb–Pb collisions at 5.02 TeV and 2.76 TeV, are presented in Fig. 1 (b) and (c). Various hydrodynamic calculations are also presented [25, 27]. The statistical and systematic uncertainties are summed in quadrature (the systematic uncertainty is smaller than the statistical uncertainty, which is typically within 5%). Data points are shifted for visibility.

the measurements.

In this Letter, we report the anisotropic flow measurements obtained from two- and multi-particle cumulants, using the approach proposed in [35–37]. These two measurements have different sensitivities to flow fluctuations and non-flow effects. Non-flow effects are azimuthal correlations not associated with the symmetry planes and usually arise from resonance decays and jets. Their contributions are expected to be suppressed when using a large pseudorapidity gap between particle pairs. Thus, in this study, we require a pseudorapidity gap of $|\Delta\eta| > 1$. This observable is denoted as $v_n\{2, |\Delta\eta| > 1\}$. On the other hand, non-flow contributions to multi-particle cumulants $v_n\{4\}$, $v_n\{6\}$, $v_n\{8\}$ are found to be negligible in events with large multiplicities characteristic for heavy-ion collisions [38].

Figure 1 (a) presents the centrality dependence of v_2 , v_3 and v_4 from two- and multi-particle cumulants, integrated over the p_T range $0.2 < p_T < 5.0$ GeV/ c , for 2.76 and 5.02 TeV Pb–Pb collisions. To elucidate the energy evolution of v_2 , v_3 and v_4 , the ratios of anisotropic flow measured at 5.02 TeV to 2.76 TeV are presented in Fig 1. (b) and (c). Assuming that non-flow effects are suppressed by the pseudorapidity gap, the remaining differences between two- and multi-particle cumulants of v_2 can be related to the strength of elliptic flow fluctuations, which are expected to give a positive and a negative contribution to the two- and multi-particle cumulant estimates, respectively [11]. Moreover, the multi-particle cumulants $v_2\{4\}$,

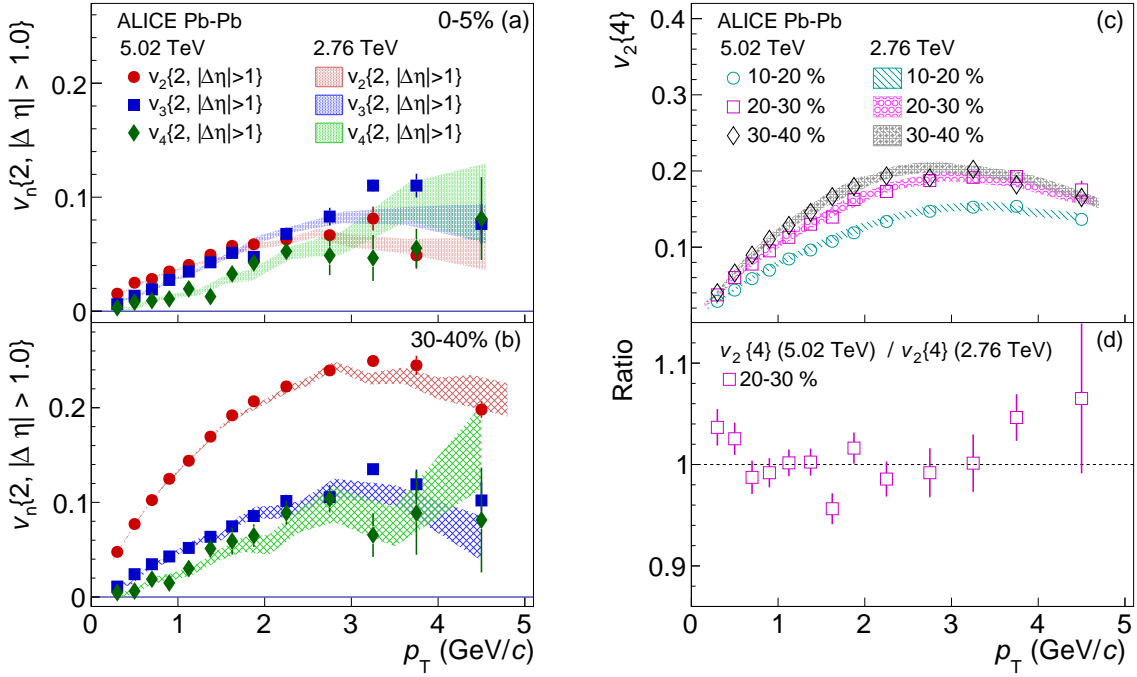


Fig. 2: (color online) $v_n(p_T)$ using two-particle cumulant method with $|\Delta\eta| > 1$ for (a) 0–5% and (b) 30–40% centrality classes; (c) $v_2(p_T)$ using four-particle cumulant method for the centrality 10–20%, 20–30% and 30–40%. Measurements for Pb–Pb collisions at $\sqrt{s_{\text{NN}}} = 2.76$ TeV are also presented as shading. (d) The ratio of $v_2\{4\}$ in 20–30% from two collision energies is also shown here. The statistical and systematical uncertainties are summed in quadrature (the systematic uncertainty is smaller than the statistical uncertainty, which is typically within 5%).

$v_2\{6\}$ and $v_2\{8\}$ are all observed to agree within 1%, which indicates that non-flow effects are largely suppressed. It is seen that $v_2\{2, |\Delta\eta| > 1\}$ increases from central to peripheral collisions, and reaches a maximum value of 0.104 ± 0.001 (stat.) ± 0.002 (syst.) in the 40–50% centrality class. For the higher harmonics, i.e. v_3 and v_4 , the values are smaller and the centrality dependence is much weaker.

Furthermore, the predictions of anisotropic flow coefficients v_n from the previously mentioned hydrodynamic model [27] are compared to the measurements in Fig. 1. (a). These predictions combine the changes in initial spatial anisotropy and the hydrodynamic response (treated as systematic uncertainty and shown by the width of the bands). The predictions are compatible with the measured anisotropic flow v_n coefficients. At the same time, a different hydrodynamic calculation [25], which employs both constant $\eta/s = 0.20$ and temperature dependent η/s , can also describe the increase in anisotropic flow measurements of v_2 (shown in Fig 1. (b)), v_3 and v_4 (see Fig 1. (c)). In particular, among the different scenarios proposed in [25], the measurements seem to favor a constant η/s going from $\sqrt{s_{\text{NN}}} = 2.76$ to 5.02 TeV Pb–Pb collisions.

The increase of v_2 and v_3 from the two energies is rather moderate, while for v_4 it is more pronounced. In addition, none of the ratios of flow harmonics exhibit a significant centrality dependence in the centrality range 0–50%, and thus the results of a fit with a constant value over these ratios are reported. An increase of $(3.0 \pm 0.6)\%$, $(4.3 \pm 1.4)\%$ and $(10.2 \pm 3.8)\%$, is obtained for elliptic, triangular and quadrangular flow, respectively, over the centrality range 0–50% in Pb–Pb collisions when going from 2.76 TeV to 5.02 TeV. This increase of anisotropic flow is compatible with theoretical predictions described in [25, 27]. Overall, these measurements support a low value of η/s for the system created in Pb–Pb collisions at $\sqrt{s_{\text{NN}}} = 5.02$ TeV and seem to indicate that it does not increase significantly with respect to Pb–Pb collisions at

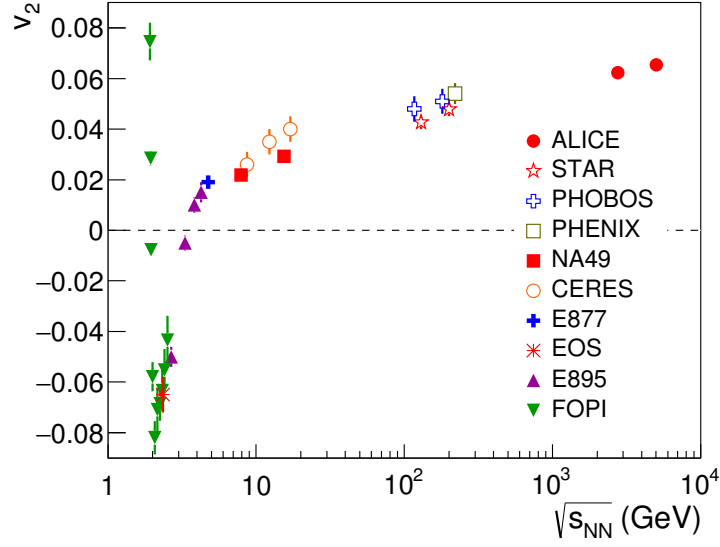


Fig. 3: Integrated elliptic flow ($v_2\{4\}$) for the 20–30% most central Pb–Pb collisions at $\sqrt{s_{\text{NN}}} = 5.02$ TeV compared with v_2 measurements at lower energies with similar centralities (see [13] for references to all data points).

$$\sqrt{s_{\text{NN}}} = 2.76 \text{ TeV.}$$

The anisotropic flow coefficients $v_2\{2, |\Delta\eta| > 1\}$, $v_3\{2, |\Delta\eta| > 1\}$ and $v_4\{2, |\Delta\eta| > 1\}$ as a function of transverse momentum (p_T) are presented in Fig. 2 for the 0–5% and 30–40% centrality classes. For the 0–5% centrality class, at $p_T > 2$ GeV/c $v_3\{2\}$ is observed to become larger than $v_2\{2\}$, while $v_4\{2\}$ is compatible with $v_2\{2\}$, within uncertainties. For the 30–40% centrality class, we see that $v_2\{2\}$ is higher than $v_3\{2\}$ and $v_4\{2\}$ for the entire p_T range measured, with no crossing of the different order flow coefficients observed. Figure 2 (c) presents the p_T -differential $v_2\{4\}$ for the 10–20%, 20–30% and 30–40% centrality classes. The $v_2\{4\}$ decreases from mid-central to central collisions over the p_T range measured. The comparison with the corresponding measurements from Pb–Pb collisions at $\sqrt{s_{\text{NN}}} = 2.76$ TeV exhibits comparable values, as illustrated by the ratio of $v_2\{4\}$ for the two energies in Fig. 2 (d). This indicates that the increase observed in the p_T integrated flow results seen in Fig. 1 can be attributed to an increase of mean transverse momentum $\langle p_T \rangle$. The measurements of p_T -differential flow are more sensitive to initial conditions and η/s , and are expected to provide important information to constrain further details of the theoretical calculations, e.g. determination of radial flow and freeze-out conditions.

Figure 3 presents the comparison of the fully p_T integrated v_2 measured in the 20–30% centrality in Pb–Pb collisions at the LHC with results at lower energies. This integrated value in the full p_T range is determined using two methods. The first uses fits to the efficiency-corrected charged-particle spectra and the p_T -differential $v_2\{4\}$ presented in Fig. 2, extrapolated to $p_T = 0$. The error on the integrated v_2 is estimated both from the uncertainty on the p_T -differential measurements and from different parameterizations that provide a good fit of the data. The second calculates $v_2\{4\}$ using tracklets formed from SPD hits in the ITS, which have an acceptance of $p_T \gtrsim 50$ MeV/c. As each method uses different ALICE sub-detectors, they can provide independent measurements of v_2 coefficients. For this centrality range, they agree within 1% for both energies. The values presented in the figure are weighted averages of these two measurements, using the inverse of the variance of each of them as weights. A continuous increase of anisotropic flow for this centrality has been observed from SPS/RHIC to LHC energies. For these fully p_T integrated coefficients, an increase of $4.9 \pm 1.9\%$ is observed going from $\sqrt{s_{\text{NN}}} = 2.76$ to 5.02

TeV, which is close to values of the previously-mentioned hydrodynamic calculations [25, 27].

In summary, we have presented the first anisotropic flow measurements of charged particles in Pb–Pb collisions at $\sqrt{s_{\text{NN}}} = 5.02$ TeV at the LHC. An average increase of $(3.0 \pm 0.6)\%$, $(4.3 \pm 1.4)\%$ and $(10.2 \pm 3.8)\%$, is observed for the transverse momentum integrated elliptic, triangular and quadrangular flow, respectively, over the centrality range 0–50% going from 2.76 TeV to 5.02 TeV. The transverse momentum dependence of anisotropic flow has also been investigated, and does not change appreciably between the two LHC energies. Therefore, the increase in integrated flow coefficients can be attributed mostly to an increase in average transverse momentum. The measurements are found to be compatible with predictions from hydrodynamic models [25, 27]. Further comparisons of p_{T} -differential flow measurements and theoretical calculations, which are not available at the time of writing, will provide extra constraints on the initial conditions and the transport properties of the QGP.

Acknowledgements

The ALICE Collaboration would like to thank all its engineers and technicians for their invaluable contributions to the construction of the experiment and the CERN accelerator teams for the outstanding performance of the LHC complex. The ALICE Collaboration gratefully acknowledges the resources and support provided by all Grid centres and the Worldwide LHC Computing Grid (WLCG) collaboration. The ALICE Collaboration acknowledges the following funding agencies for their support in building and running the ALICE detector: State Committee of Science, World Federation of Scientists (WFS) and Swiss Fonds Kidagan, Armenia; Conselho Nacional de Desenvolvimento Científico e Tecnológico (CNPq), Financiadora de Estudos e Projetos (FINEP), Fundação de Amparo à Pesquisa do Estado de São Paulo (FAPESP); National Natural Science Foundation of China (NSFC), the Chinese Ministry of Education (CMOE) and the Ministry of Science and Technology of China (MSTC); Ministry of Education and Youth of the Czech Republic; Danish Natural Science Research Council, the Carlsberg Foundation and the Danish National Research Foundation; The European Research Council under the European Community’s Seventh Framework Programme; Helsinki Institute of Physics and the Academy of Finland; French CNRS-IN2P3, the ‘Region Pays de Loire’, ‘Region Alsace’, ‘Region Auvergne’ and CEA, France; German Bundesministerium für Bildung, Wissenschaft, Forschung und Technologie (BMBF) and the Helmholtz Association; General Secretariat for Research and Technology, Ministry of Development, Greece; National Research, Development and Innovation Office (NKFIH), Hungary; Department of Atomic Energy and Department of Science and Technology of the Government of India; Istituto Nazionale di Fisica Nucleare (INFN) and Centro Fermi - Museo Storico della Fisica e Centro Studi e Ricerche “Enrico Fermi”, Italy; Japan Society for the Promotion of Science (JSPS) KAKENHI and MEXT, Japan; Joint Institute for Nuclear Research, Dubna; National Research Foundation of Korea (NRF); Consejo Nacional de Ciencia y Tecnología (CONACYT), Dirección General de Asuntos del Personal Académico (DGAPA), México, Amérique Latine Formation académique - European Commission (ALFA-EC) and the EPLANET Program (European Particle Physics Latin American Network); Stichting voor Fundamenteel Onderzoek der Materie (FOM) and the Nederlandse Organisatie voor Wetenschappelijk Onderzoek (NWO), Netherlands; Research Council of Norway (NFR); National Science Centre, Poland; Ministry of National Education/Institute for Atomic Physics and National Council of Scientific Research in Higher Education (CNCSI-UEFISCDI), Romania; Ministry of Education and Science of Russian Federation, Russian Academy of Sciences, Russian Federal Agency of Atomic Energy, Russian Federal Agency for Science and Innovations and The Russian Foundation for Basic Research; Ministry of Education of Slovakia; Department of Science and Technology, South Africa; Centro de Investigaciones Energéticas, Medioambientales y Tecnológicas (CIEMAT), E-Infrastructure shared between Europe and Latin America (EELA), Ministerio de Economía y Competitividad (MINECO) of Spain, Xunta de Galicia (Consellería de Educación), Centro de Aplicaciones Tecnológicas y Desarrollo Nuclear (CEADEN), Cubaenergía, Cuba, and IAEA (International Atomic Energy Agency); Swedish

Research Council (VR) and Knut & Alice Wallenberg Foundation (KAW); Ukraine Ministry of Education and Science; United Kingdom Science and Technology Facilities Council (STFC); The United States Department of Energy, the United States National Science Foundation, the State of Texas, and the State of Ohio; Ministry of Science, Education and Sports of Croatia and Unity through Knowledge Fund, Croatia; Council of Scientific and Industrial Research (CSIR), New Delhi, India; Pontificia Universidad Católica del Perú.

References

- [1] S. Borsanyi, G. Endrodi, Z. Fodor, A. Jakovac, S. D. Katz, S. Krieg, C. Ratti, and K. K. Szabo, “The QCD equation of state with dynamical quarks,” *JHEP* **11** (2010) 077, arXiv:1007.2580 [hep-lat].
- [2] **HotQCD** Collaboration, A. Bazavov *et al.*, “Equation of state in (2+1)-flavor QCD,” *Phys. Rev. D* **90** (2014) 094503, arXiv:1407.6387 [hep-lat].
- [3] **ALICE** Collaboration, K. Aamodt *et al.*, “Centrality dependence of the charged-particle multiplicity density at mid-rapidity in Pb-Pb collisions at $\sqrt{s_{NN}} = 2.76$ TeV,” *Phys. Rev. Lett.* **106** (2011) 032301, arXiv:1012.1657 [nucl-ex].
- [4] **ALICE** Collaboration, J. Adam *et al.*, “Centrality dependence of the charged-particle multiplicity density at mid-rapidity in Pb-Pb collisions at $\sqrt{s_{NN}} = 5.02$ TeV,” arXiv:1512.06104 [nucl-ex].
- [5] G. Odyniec, “RHIC Beam Energy Scan Program: Phase I and II,” *PoS CPOD2013* (2013) 043.
- [6] **STAR** Collaboration, L. Adamczyk *et al.*, “Inclusive charged hadron elliptic flow in Au + Au collisions at $\sqrt{s_{NN}} = 7.7 - 39$ GeV,” *Phys. Rev. C* **86** (2012) 054908, arXiv:1206.5528 [nucl-ex].
- [7] **PHENIX** Collaboration, S. S. Adler *et al.*, “Transverse-energy distributions at midrapidity in p+p, d+Au, and Au+Au collisions at $\sqrt{s_{NN}} = 62.4 - 200$ GeV and implications for particle-production models,” *Phys. Rev. C* **89** no. 4, (2014) 044905, arXiv:1312.6676 [nucl-ex].
- [8] R. V. Gavai and S. Gupta, “The Critical end point of QCD,” *Phys. Rev. D* **71** (2005) 114014, arXiv:hep-lat/0412035 [hep-lat].
- [9] P. Braun-Munzinger, V. Koch, T. Schaefer, and J. Stachel, “Properties of hot and dense matter from relativistic heavy ion collisions,” arXiv:1510.00442 [nucl-th].
- [10] J.-Y. Ollitrault, “Anisotropy as a signature of transverse collective flow,” *Phys. Rev. D* **46** (1992) 229–245.
- [11] S. A. Voloshin, A. M. Poskanzer, and R. Snellings, “Collective phenomena in non-central nuclear collisions,” arXiv:0809.2949 [nucl-ex].
- [12] S. Voloshin and Y. Zhang, “Flow study in relativistic nuclear collisions by Fourier expansion of Azimuthal particle distributions,” *Z. Phys. C* **70** (1996) 665–672, arXiv:hep-ph/9407282 [hep-ph].
- [13] **ALICE** Collaboration, K. Aamodt *et al.*, “Elliptic flow of charged particles in Pb-Pb collisions at $\sqrt{s_{NN}} = 2.76$ TeV,” *Phys. Rev. Lett.* **105** (2010) 252302, arXiv:1011.3914 [nucl-ex].
- [14] **STAR** Collaboration, K. H. Ackermann *et al.*, “Elliptic flow in Au + Au collisions at $\sqrt{s_{NN}} = 130$ GeV,” *Phys. Rev. Lett.* **86** (2001) 402–407, arXiv:nucl-ex/0009011 [nucl-ex].

- [15] M. Luzum and P. Romatschke, “Viscous Hydrodynamic Predictions for Nuclear Collisions at the LHC,” *Phys. Rev. Lett.* **103** (2009) 262302, arXiv:0901.4588 [nucl-th].
- [16] T. Hirano, P. Huovinen, and Y. Nara, “Elliptic flow in U+U collisions at $\sqrt{s_{NN}} = 200$ GeV and in Pb+Pb collisions at $\sqrt{s_{NN}} = 2.76$ TeV: Prediction from a hybrid approach,” *Phys. Rev.* **C83** (2011) 021902, arXiv:1010.6222 [nucl-th].
- [17] T. Hirano, U. W. Heinz, D. Kharzeev, R. Lacey, and Y. Nara, “Hadronic dissipative effects on elliptic flow in ultrarelativistic heavy-ion collisions,” *Phys. Lett.* **B636** (2006) 299–304, arXiv:nucl-th/0511046 [nucl-th].
- [18] H.-J. Drescher, A. Dumitru, and J.-Y. Ollitrault, “The Centrality dependence of elliptic flow at LHC,” in *Workshop on Heavy Ion Collisions at the LHC: Last Call for Predictions Geneva, Switzerland, May 14-June 8, 2007*. 2007. arXiv:0706.1707 [nucl-th].
<https://inspirehep.net/record/752929/files/arXiv:0706.1707.pdf>.
- [19] B. Alver and G. Roland, “Collision geometry fluctuations and triangular flow in heavy-ion collisions,” *Phys. Rev.* **C81** (2010) 054905, arXiv:1003.0194 [nucl-th]. [Erratum: *Phys. Rev.* **C82**,039903(2010)].
- [20] ALICE Collaboration, K. Aamodt *et al.*, “Higher harmonic anisotropic flow measurements of charged particles in Pb-Pb collisions at $\sqrt{s_{NN}}=2.76$ TeV,” *Phys. Rev. Lett.* **107** (2011) 032301, arXiv:1105.3865 [nucl-ex].
- [21] ATLAS Collaboration, G. Aad *et al.*, “Measurement of the azimuthal anisotropy for charged particle production in $\sqrt{s_{NN}} = 2.76$ TeV lead-lead collisions with the ATLAS detector,” *Phys. Rev.* **C86** (2012) 014907, arXiv:1203.3087 [hep-ex].
- [22] CMS Collaboration, S. Chatrchyan *et al.*, “Measurement of higher-order harmonic azimuthal anisotropy in PbPb collisions at $\sqrt{s_{NN}} = 2.76$ TeV,” *Phys. Rev.* **C89** no. 4, (2014) 044906, arXiv:1310.8651 [nucl-ex].
- [23] ATLAS Collaboration, G. Aad *et al.*, “Measurement of event-plane correlations in $\sqrt{s_{NN}} = 2.76$ TeV lead-lead collisions with the ATLAS detector,” *Phys. Rev.* **C90** no. 2, (2014) 024905, arXiv:1403.0489 [hep-ex].
- [24] P. Kovtun, D. T. Son, and A. O. Starinets, “Viscosity in strongly interacting quantum field theories from black hole physics,” *Phys. Rev. Lett.* **94** (2005) 111601, arXiv:hep-th/0405231 [hep-th].
- [25] H. Niemi, K. J. Eskola, R. Paatelainen, and K. Tuominen, “Predictions for 5.023 TeV Pb+Pb collisions at the LHC,” arXiv:1511.04296 [hep-ph].
- [26] N. Borghini, P. M. Dinh, and J.-Y. Ollitrault, “A New method for measuring azimuthal distributions in nucleus-nucleus collisions,” *Phys. Rev.* **C63** (2001) 054906, arXiv:nucl-th/0007063 [nucl-th].
- [27] J. Noronha-Hostler, M. Luzum, and J.-Y. Ollitrault, “Hydrodynamic predictions for 5.02 TeV Pb-Pb collisions,” arXiv:1511.06289 [nucl-th].
- [28] C. Shen and U. Heinz, “Collision Energy Dependence of Viscous Hydrodynamic Flow in Relativistic Heavy-Ion Collisions,” *Phys. Rev.* **C85** (2012) 054902, arXiv:1202.6620 [nucl-th]. [Erratum: *Phys. Rev.* **C86**,049903(2012)].
- [29] J. Auvinen and H. Petersen, “Evolution of elliptic and triangular flow as a function of beam energy in a hybrid model,” *J. Phys. Conf. Ser.* **503** (2014) 012025, arXiv:1310.7751 [nucl-th].

- [30] ALICE Collaboration, K. Aamodt *et al.*, “The ALICE experiment at the CERN LHC,” *JINST* **3** (2008) S08002.
- [31] ALICE Collaboration, P. Cortese *et al.*, “ALICE: Physics performance report, volume II,” *J. Phys.* **G32** (2006) 1295–2040.
- [32] ALICE Collaboration, B. Abelev *et al.*, “Centrality determination of Pb-Pb collisions at $\sqrt{s_{NN}} = 2.76$ TeV with ALICE,” *Phys. Rev.* **C88** no. 4, (2013) 044909, arXiv:1301.4361 [nucl-ex].
- [33] X.-N. Wang and M. Gyulassy, “HIJING: A Monte Carlo model for multiple jet production in p p, p A and A A collisions,” *Phys. Rev.* **D44** (1991) 3501–3516.
- [34] R. Brun, F. Carminati, and S. Giani, “GEANT Detector Description and Simulation Tool,” 1994. <https://cds.cern.ch/record/118715?ln=en>.
- [35] Y. Zhou, X. Zhu, P. Li, and H. Song, “Investigation of possible hadronic flow in $\sqrt{s_{NN}} = 5.02$ TeV p – Pb collisions,” *Phys. Rev.* **C91** (2015) 064908, arXiv:1503.06986 [nucl-th].
- [36] A. Bilandzic, R. Snellings, and S. Voloshin, “Flow analysis with cumulants: Direct calculations,” *Phys. Rev.* **C83** (2011) 044913, arXiv:1010.0233 [nucl-ex].
- [37] A. Bilandzic, C. H. Christensen, K. Gulbrandsen, A. Hansen, and Y. Zhou, “Generic framework for anisotropic flow analyses with multiparticle azimuthal correlations,” *Phys. Rev.* **C89** no. 6, (2014) 064904, arXiv:1312.3572 [nucl-ex].
- [38] ALICE Collaboration, B. B. Abelev *et al.*, “Multiparticle azimuthal correlations in p -Pb and Pb-Pb collisions at the CERN Large Hadron Collider,” *Phys. Rev.* **C90** no. 5, (2014) 054901, arXiv:1406.2474 [nucl-ex].

A The ALICE Collaboration

J. Adam³⁹, D. Adamová⁸⁴, M.M. Aggarwal⁸⁸, G. Aglieri Rinella³⁵, M. Agnello¹¹⁰, N. Agrawal⁴⁷, Z. Ahammed¹³², S. Ahmad¹⁹, S.U. Ahn⁶⁸, S. Aiola¹³⁶, A. Akindinov⁵⁸, S.N. Alam¹³², D.S.D. Albuquerque¹²¹, D. Aleksandrov⁸⁰, B. Alessandro¹¹⁰, D. Alexandre¹⁰¹, R. Alfaro Molina⁶⁴, A. Alici^{104,12}, A. Alkin³, J.R.M. Almaraz¹¹⁹, J. Alme³⁷, T. Alt⁴², S. Altinpinar¹⁸, I. Altsybeev¹³¹, C. Alves Garcia Prado¹²⁰, C. Andrei⁷⁸, A. Andronic⁹⁷, V. Anguelov⁹⁴, T. Antičić⁹⁸, F. Antinori¹⁰⁷, P. Antonioli¹⁰⁴, L. Aphecetche¹¹³, H. Appelshäuser⁵³, S. Arcelli²⁷, R. Arnaldi¹¹⁰, O.W. Arnold^{36,93}, I.C. Arsene²², M. Arslandok⁵³, B. Audurier¹¹³, A. Augustinus³⁵, R. Averbeck⁹⁷, M.D. Azmi¹⁹, A. Badalà¹⁰⁶, Y.W. Baek⁶⁷, S. Bagnasco¹¹⁰, R. Bailhache⁵³, R. Bala⁹¹, S. Balasubramanian¹³⁶, A. Baldissieri¹⁵, R.C. Baral⁶¹, A.M. Barbano²⁶, R. Barbera²⁸, F. Barile³², G.G. Barnaföldi¹³⁵, L.S. Barnby¹⁰¹, V. Barret⁷⁰, P. Bartalini⁷, K. Barth³⁵, J. Bartke¹¹⁷, E. Bartsch⁵³, M. Basile²⁷, N. Bastid⁷⁰, S. Basu¹³², B. Bathen⁵⁴, G. Batigne¹¹³, A. Batista Camejo⁷⁰, B. Batyunya⁶⁶, P.C. Batzing²², I.G. Bearden⁸¹, H. Beck⁵³, C. Bedda¹¹⁰, N.K. Behera^{50,48}, I. Belikov⁵⁵, F. Bellini²⁷, H. Bello Martinez², R. Bellwied¹²², R. Belmont¹³⁴, E. Belmont-Moreno⁶⁴, V. Belyaev⁷⁵, P. Benacek⁸⁴, G. Bencedi¹³⁵, S. Beole²⁶, I. Berceau⁷⁸, A. Bercuci⁷⁸, Y. Berdnikov⁸⁶, D. Berenyi¹³⁵, R.A. Bertens⁵⁷, D. Berzano³⁵, L. Betev³⁵, A. Bhasin⁹¹, I.R. Bhat⁹¹, A.K. Bhati⁸⁸, B. Bhattacharjee⁴⁴, J. Bhom^{128,117}, L. Bianchi¹²², N. Bianchi⁷², C. Bianchin¹³⁴, J. Bielčik³⁹, J. Bielčíková⁸⁴, A. Bilandžić^{81,36,93}, G. Biro¹³⁵, R. Biswas⁴, S. Biswas^{4,79}, S. Bjelogrić⁵⁷, J.T. Blair¹¹⁸, D. Blau⁸⁰, C. Blume⁵³, F. Bock^{74,94}, A. Bogdanov⁷⁵, H. Bøggild⁸¹, L. Boldizsár¹³⁵, M. Bombara⁴⁰, J. Book⁵³, H. Borel¹⁵, A. Borissov⁹⁶, M. Borri^{83,124}, F. Bossú⁶⁵, E. Botta²⁶, C. Bourjau⁸¹, P. Braun-Munzinger⁹⁷, M. Bregant¹²⁰, T. Breitner⁵², T.A. Broker⁵³, T.A. Browning⁹⁵, M. Broz³⁹, E.J. Brucken⁴⁵, E. Bruna¹¹⁰, G.E. Bruno³², D. Budnikov⁹⁹, H. Buesching⁵³, S. Bufalino^{35,26}, P. Buncic³⁵, O. Busch^{94,128}, Z. Buthelezi⁶⁵, J.B. Butt¹⁶, J.T. Buxton²⁰, J. Cabala¹¹⁵, D. Caffarri³⁵, X. Cai⁷, H. Caines¹³⁶, L. Calero Diaz⁷², A. Caliva⁵⁷, E. Calvo Villar¹⁰², P. Camerini²⁵, F. Carena³⁵, W. Carena³⁵, F. Carnesecchi²⁷, J. Castillo Castellanos¹⁵, A.J. Castro¹²⁵, E.A.R. Casula²⁴, C. Ceballos Sanchez⁹, J. Cepila³⁹, P. Cerello¹¹⁰, J. Cerkala¹¹⁵, B. Chang¹²³, S. Chapeland³⁵, M. Chartier¹²⁴, J.L. Charvet¹⁵, S. Chattopadhyay¹³², S. Chattopadhyay¹⁰⁰, A. Chauvin^{93,36}, V. Chelnokov³, M. Cherney⁸⁷, C. Cheshkov¹³⁰, B. Cheynis¹³⁰, V. Chibante Barroso³⁵, D.D. Chinellato¹²¹, S. Cho⁵⁰, P. Chochula³⁵, K. Choi⁹⁶, M. Chojnacki⁸¹, S. Choudhury¹³², P. Christakoglou⁸², C.H. Christensen⁸¹, P. Christiansen³³, T. Chujo¹²⁸, S.U. Chung⁹⁶, C. Cicalo¹⁰⁵, L. Cifarelli^{12,27}, F. Cindolo¹⁰⁴, J. Cleymans⁹⁰, F. Colamaria³², D. Colella^{59,35}, A. Collu^{74,24}, M. Colocci²⁷, G. Conesa Balbastre⁷¹, Z. Conesa del Valle⁵¹, M.E. Connors^{ii,136}, J.G. Contreras³⁹, T.M. Cormier⁸⁵, Y. Corrales Morales¹¹⁰, I. Cortés Maldonado², P. Cortese³¹, M.R. Cosentino¹²⁰, F. Costa³⁵, P. Crochet⁷⁰, R. Cruz Albino¹¹, E. Cuautle⁶³, L. Cunqueiro^{54,35}, T. Dahms^{93,36}, A. Dainese¹⁰⁷, M.C. Danisch⁹⁴, A. Danu⁶², D. Das¹⁰⁰, I. Das¹⁰⁰, S. Das⁴, A. Dash⁷⁹, S. Dash⁴⁷, S. De¹²⁰, A. De Caro^{12,30}, G. de Cataldo¹⁰³, C. de Conti¹²⁰, J. de Cuveland⁴², A. De Falco²⁴, D. De Gruttola^{12,30}, N. De Marco¹¹⁰, S. De Pasquale³⁰, A. Deisting^{97,94}, A. Deloff⁷⁷, E. Dénes^{135,i}, C. Deplano⁸², P. Dhankher⁴⁷, D. Di Bari³², A. Di Mauro³⁵, P. Di Nezza⁷², M.A. Diaz Corchero¹⁰, T. Dietel⁹⁰, P. Dillenseger⁵³, R. Divià³⁵, Ø. Djuvslund¹⁸, A. Dobrin^{82,62}, D. Domenicis Gimenez¹²⁰, B. Dönigus⁵³, O. Dordic²², T. Drozhzhova⁵³, A.K. Dubey¹³², A. Dubla⁵⁷, L. Ducroux¹³⁰, P. Dupieux⁷⁰, R.J. Ehlers¹³⁶, D. Elia¹⁰³, E. Endress¹⁰², H. Engel⁵², E. Epple¹³⁶, B. Erasmus¹¹³, I. Erdemir⁵³, F. Erhardt¹²⁹, B. Espagnon⁵¹, M. Estienne¹¹³, S. Esumi¹²⁸, J. Eum⁹⁶, D. Evans¹⁰¹, S. Evdokimov¹¹¹, G. Eyyubova³⁹, L. Fabbietti^{93,36}, D. Fabris¹⁰⁷, J. Faivre⁷¹, A. Fantoni⁷², M. Fasel⁷⁴, L. Feldkamp⁵⁴, A. Feliciello¹¹⁰, G. Feofilov¹³¹, J. Ferencei⁸⁴, A. Fernández Téllez², E.G. Ferreira¹⁷, A. Ferretti²⁶, A. Festanti²⁹, V.J.G. Feuillard^{15,70}, J. Figiel¹¹⁷, M.A.S. Figueredo^{124,120}, S. Filchagin⁹⁹, D. Finogeev⁵⁶, F.M. Fionda²⁴, E.M. Fiore³², M.G. Fleck⁹⁴, M. Floris³⁵, S. Foertsch⁶⁵, P. Foka⁹⁷, S. Fokin⁸⁰, E. Fragiaco¹⁰⁹, A. Francescon^{35,29}, U. Frankendorf⁹⁷, G.G. Fronze²⁶, U. Fuchs³⁵, C. Furget⁷¹, A. Furs⁵⁶, M. Fusco Girard³⁰, J.J. Gaardhøje⁸¹, M. Gagliardi²⁶, A.M. Gago¹⁰², M. Gallio²⁶, D.R. Gangadharan⁷⁴, P. Ganoti⁸⁹, C. Gao⁷, C. Garabatos⁹⁷, E. Garcia-Solis¹³, C. Gargiulo³⁵, P. Gasik^{93,36}, E.F. Gauger¹¹⁸, M. Germain¹¹³, A. Gheata³⁵, M. Gheata^{35,62}, P. Ghosh¹³², S.K. Ghosh⁴, P. Gianotti⁷², P. Giubellino^{110,35}, P. Giubilato²⁹, E. Gladysz-Dziadus¹¹⁷, P. Glässel⁹⁴, D.M. Gómez Coral⁶⁴, A. Gomez Ramirez⁵², A.S. Gonzalez³⁵, V. Gonzalez¹⁰, P. González-Zamora¹⁰, S. Gorbunov⁴², L. Görlich¹¹⁷, S. Gotovac¹¹⁶, V. Grabski⁶⁴, O.A. Grachov¹³⁶, L.K. Graczykowski¹³³, K.L. Graham¹⁰¹, A. Grelli⁵⁷, A. Grigoras³⁵, C. Grigoras³⁵, V. Grigoriev⁷⁵, A. Grigoryan¹, S. Grigoryan⁶⁶, B. Grinyov³, N. Grion¹⁰⁹, J.M. Gronefeld⁹⁷, J.F. Grosse-Oetringhaus³⁵, R. Grosso⁹⁷, F. Guber⁵⁶, R. Guernane⁷¹, B. Guerzoni²⁷, K. Gulbrandsen⁸¹, T. Gunji¹²⁷, A. Gupta⁹¹, R. Gupta⁹¹, R. Haake⁵⁴, Ø. Haaland¹⁸, C. Hadjidakis⁵¹, M. Haiduc⁶², H. Hamagaki¹²⁷, G. Hamar¹³⁵, J.C. Hamon⁵⁵, J.W. Harris¹³⁶, A. Harton¹³, D. Hatzifotiadou¹⁰⁴, S. Hayashi¹²⁷, S.T. Heckel⁵³, E. Hellbär⁵³, H. Helstrup³⁷, A. Hergelegiu⁷⁸, G. Herrera Corral¹¹, B.A. Hess³⁴, K.F. Hetland³⁷, H. Hillemanns³⁵, B. Hippolyte⁵⁵, D. Horak³⁹, R. Hosokawa¹²⁸, P. Hristov³⁵, T.J. Humanic²⁰,

N. Hussain⁴⁴, T. Hussain¹⁹, D. Hutter⁴², D.S. Hwang²¹, R. Ilkaev⁹⁹, M. Inaba¹²⁸, E. Incani²⁴, M. Ippolitov^{75,80}, M. Irfan¹⁹, M. Ivanov⁹⁷, V. Ivanov⁸⁶, V. Izucheev¹¹¹, N. Jacazio²⁷, P.M. Jacobs⁷⁴, M.B. Jadhav⁴⁷, S. Jadlovská¹¹⁵, J. Jadlovsky^{115,59}, C. Jahnke¹²⁰, M.J. Jakubowska¹³³, H.J. Jang⁶⁸, M.A. Janik¹³³, P.H.S.Y. Jayarathna¹²², C. Jena²⁹, S. Jena¹²², R.T. Jimenez Bustamante⁹⁷, P.G. Jones¹⁰¹, A. Jusko¹⁰¹, P. Kalinak⁵⁹, A. Kalweit³⁵, J. Kamin⁵³, J.H. Kang¹³⁷, V. Kaplin⁷⁵, S. Kar¹³², A. Karasu Uysal⁶⁹, O. Karavichev⁵⁶, T. Karavicheva⁵⁶, L. Karayan^{97,94}, E. Karpechev⁵⁶, U. Kebschull⁵², R. Keidel¹³⁸, D.L.D. Keijdener⁵⁷, M. Keil³⁵, M. Mohisin Khan^{iii,19}, P. Khan¹⁰⁰, S.A. Khan¹³², A. Khanzadeev⁸⁶, Y. Kharlov¹¹¹, B. Kileng³⁷, D.W. Kim⁴³, D.J. Kim¹²³, D. Kim¹³⁷, H. Kim¹³⁷, J.S. Kim⁴³, M. Kim¹³⁷, S. Kim²¹, T. Kim¹³⁷, S. Kirsch⁴², I. Kisel⁴², S. Kiselev⁵⁸, A. Kisiel¹³³, G. Kiss¹³⁵, J.L. Klay⁶, C. Klein⁵³, J. Klein³⁵, C. Klein-Bösing⁵⁴, S. Klewin⁹⁴, A. Kluge³⁵, M.L. Knichel⁹⁴, A.G. Knospe^{118,122}, C. Kobdaj¹¹⁴, M. Kofarago³⁵, T. Kollegger⁹⁷, A. Kolojvari¹³¹, V. Kondratiev¹³¹, N. Kondratyeva⁷⁵, E. Kondratyuk¹¹¹, A. Konevskikh⁵⁶, M. Kopcik¹¹⁵, P. Kostarakis⁸⁹, M. Kour⁹¹, C. Kouzinopoulos³⁵, O. Kovalenko⁷⁷, V. Kovalenko¹³¹, M. Kowalski¹¹⁷, G. Koyithatta Meethalevedu⁴⁷, I. Králik⁵⁹, A. Kravčáková⁴⁰, M. Krivda^{59,101}, F. Krizek⁸⁴, E. Kryshen^{86,35}, M. Krzewicki⁴², A.M. Kubera²⁰, V. Kučera⁸⁴, C. Kuhn⁵⁵, P.G. Kuijjer⁸², A. Kumar⁹¹, J. Kumar⁴⁷, L. Kumar⁸⁸, S. Kumar⁴⁷, P. Kurashvili⁷⁷, A. Kurepin⁵⁶, A.B. Kurepin⁵⁶, A. Kuryakin⁹⁹, M.J. Kweon⁵⁰, Y. Kwon¹³⁷, S.L. La Pointe¹¹⁰, P. La Rocca²⁸, P. Ladrón de Guevara¹¹, C. Lagana Fernandes¹²⁰, I. Lakomov³⁵, R. Langoy⁴¹, C. Lara⁵², A. Lardeux¹⁵, A. Lattuca²⁶, E. Laudi³⁵, R. Lea²⁵, L. Leardini⁹⁴, G.R. Lee¹⁰¹, S. Lee¹³⁷, F. Lehas⁸², R.C. Lemmon⁸³, V. Lenti¹⁰³, E. Leogrande⁵⁷, I. León Monzón¹¹⁹, H. León Vargas⁶⁴, M. Leoncino²⁶, P. Lévai¹³⁵, S. Li^{7,70}, X. Li¹⁴, J. Lien⁴¹, R. Lietava¹⁰¹, S. Lindal²², V. Lindenstruth⁴², C. Lippmann⁹⁷, M.A. Lisa²⁰, H.M. Ljunggren³³, D.F. Lodato⁵⁷, P.I. Loenne¹⁸, V. Loginov⁷⁵, C. Loizides⁷⁴, X. Lopez⁷⁰, E. López Torres⁹, A. Lowe¹³⁵, P. Luettig⁵³, M. Lunardon²⁹, G. Luparello²⁵, T.H. Lutz¹³⁶, A. Maevskaya⁵⁶, M. Mager³⁵, S. Mahajan⁹¹, S.M. Mahmood²², A. Maire⁵⁵, R.D. Majka¹³⁶, M. Malaev⁸⁶, I. Maldonado Cervantes⁶³, L. Malinina^{iv,66}, D. Mal'Kevich⁵⁸, P. Malzacher⁹⁷, A. Mamonov⁹⁹, V. Manko⁸⁰, F. Manso⁷⁰, V. Manzari^{103,35}, M. Marchisone^{65,126,26}, J. Mareš⁶⁰, G.V. Margagliotti²⁵, A. Margotti¹⁰⁴, J. Margutti⁵⁷, A. Marín⁹⁷, C. Markert¹¹⁸, M. Marquard⁵³, N.A. Martin⁹⁷, J. Martin Blanco¹¹³, P. Martinengo³⁵, M.I. Martínez², G. Martínez García¹¹³, M. Martínez Pedreira³⁵, A. Mas¹²⁰, S. Masciocchi⁹⁷, M. Maserà²⁶, A. Masoni¹⁰⁵, A. Mastroserio³², A. Matyja¹¹⁷, C. Mayer¹¹⁷, J. Mazer¹²⁵, M.A. Mazzone¹⁰⁸, D. McDonald¹²², F. Meddi²³, Y. Melikyan⁷⁵, A. Menchaca-Rocha⁶⁴, E. Meninno³⁰, J. Mercado Pérez⁹⁴, M. Meres³⁸, Y. Miake¹²⁸, M.M. Mieskolainen⁴⁵, K. Mikhaylov^{66,58}, L. Milano^{35,74}, J. Milosevic²², A. Mischke⁵⁷, A.N. Mishra⁴⁸, D. Miśkowiec⁹⁷, J. Mitra¹³², C.M. Mitu⁶², N. Mohammadi⁵⁷, B. Mohanty^{132,79}, L. Molnar^{55,113}, L. Montaño Zetina¹¹, E. Montes¹⁰, D.A. Moreira De Godoy⁵⁴, L.A.P. Moreno², S. Moretto²⁹, A. Morreale¹¹³, A. Morsch³⁵, V. Muccifora⁷², E. Mudnic¹¹⁶, D. Mühlheim⁵⁴, S. Muhuri¹³², M. Mukherjee¹³², J.D. Mulligan¹³⁶, M.G. Munhoz¹²⁰, R.H. Munzer^{93,36,53}, H. Murakami¹²⁷, S. Murray⁶⁵, L. Musa³⁵, J. Musinsky⁵⁹, B. Naik⁴⁷, R. Nair⁷⁷, B.K. Nandi⁴⁷, R. Nania¹⁰⁴, E. Nappi¹⁰³, M.U. Naru¹⁶, H. Natal da Luz¹²⁰, C. Natrass¹²⁵, S.R. Navarro², K. Nayak⁷⁹, R. Nayak⁴⁷, T.K. Nayak¹³², S. Nazarenko⁹⁹, A. Nedosekin⁵⁸, L. Nellen⁶³, F. Ng¹²², M. Nicassio⁹⁷, M. Niculescu⁶², J. Niedziela³⁵, B.S. Nielsen⁸¹, S. Nikolaev⁸⁰, S. Nikulin⁸⁰, V. Nikulin⁸⁶, F. Noferini^{104,12}, P. Nomokonov⁶⁶, G. Nooren⁵⁷, J.C.C. Noris², J. Norman¹²⁴, A. Nyman⁸⁰, J. Nystrand¹⁸, H. Oeschler⁹⁴, S. Oh¹³⁶, S.K. Oh⁶⁷, A. Ohlson³⁵, A. Okatan⁶⁹, T. Okubo⁴⁶, L. Olah¹³⁵, J. Oleniacz¹³³, A.C. Oliveira Da Silva¹²⁰, M.H. Oliver¹³⁶, J. Onderwaater⁹⁷, C. Oppedisano¹¹⁰, R. Orava⁴⁵, M. Oravec¹¹⁵, A. Ortiz Velasquez⁶³, A. Oskarsson³³, J. Otwinowski¹¹⁷, K. Oyama^{94,76}, M. Ozdemir⁵³, Y. Pachmayer⁹⁴, D. Pagano²⁶, P. Pagano³⁰, G. Paic⁶³, S.K. Pal¹³², J. Pan¹³⁴, A.K. Pandey⁴⁷, V. Papikyan¹, G.S. Pappalardo¹⁰⁶, P. Pareek⁴⁸, W.J. Park⁹⁷, S. Parmar⁸⁸, A. Passfeld⁵⁴, V. Paticchio¹⁰³, R.N. Patra¹³², B. Paul¹⁰⁰, H. Pei⁷, T. Peitzmann⁵⁷, H. Pereira Da Costa¹⁵, D. Peresunko^{80,75}, C.E. Pérez Lara⁸², E. Perez Lezama⁵³, V. Peskov⁵³, Y. Pestov⁵, V. Petráček³⁹, V. Petrov¹¹¹, M. Petrovici⁷⁸, C. Petta²⁸, S. Piano¹⁰⁹, M. Pikna³⁸, P. Pillot¹¹³, L.O.D.L. Pimentel⁸¹, O. Pinazza^{104,35}, L. Pinsky¹²², D.B. Piyarathna¹²², M. Płoskoń⁷⁴, M. Planinic¹²⁹, J. Pluta¹³³, S. Pochybova¹³⁵, P.L.M. Podesta-Lerma¹¹⁹, M.G. Poghosyan^{85,87}, B. Polichtchouk¹¹¹, N. Poljak¹²⁹, W. Poonsawat¹¹⁴, A. Pop⁷⁸, S. Porteboeuf-Houssais⁷⁰, J. Porter⁷⁴, J. Pospisil⁸⁴, S.K. Prasad⁴, R. Preghenella^{104,35}, F. Prino¹¹⁰, C.A. Pruneau¹³⁴, I. Pshenichnov⁵⁶, M. Puccio²⁶, G. Puddu²⁴, P. Pujahari¹³⁴, V. Punin⁹⁹, J. Putschke¹³⁴, H. Qvigstad²², A. Rachevski¹⁰⁹, S. Raha⁴, S. Rajput⁹¹, J. Rak¹²³, A. Rakotozafindrabe¹⁵, L. Ramello³¹, F. Rami⁵⁵, R. Raniwala⁹², S. Raniwala⁹², S.S. Räsänen⁴⁵, B.T. Rascanu⁵³, D. Rathee⁸⁸, K.F. Read^{85,125}, K. Redlich⁷⁷, R.J. Reed¹³⁴, A. Rehman¹⁸, P. Reichelt⁵³, F. Reidt^{94,35}, X. Ren⁷, R. Renfordt⁵³, A.R. Reolon⁷², A. Reshetin⁵⁶, K. Reygers⁹⁴, V. Riabov⁸⁶, R.A. Ricci⁷³, T. Richert³³, M. Richter²², P. Riedler³⁵, W. Riegler³⁵, F. Riggi²⁸, C. Ristea⁶², E. Rocco⁵⁷, M. Rodríguez Cahuantzi^{11,2}, A. Rodríguez Manso⁸², K. Røed²², E. Rogochaya⁶⁶, D. Rohr⁴², D. Röhrich¹⁸, F. Ronchetti^{72,35}, L. Ronflette¹¹³, P. Rosnet⁷⁰, A. Rossi^{35,29},

F. Roukoutakis⁸⁹, A. Roy⁴⁸, C. Roy⁵⁵, P. Roy¹⁰⁰, A.J. Rubio Montero¹⁰, R. Rui²⁵, R. Russo²⁶, E. Ryabinkin⁸⁰, Y. Ryabov⁸⁶, A. Rybicki¹¹⁷, S. Saarinen⁴⁵, S. Sadhu¹³², S. Sadvovsky¹¹¹, K. Šafařík³⁵, B. Sahlmuller⁵³, P. Sahoo⁴⁸, R. Sahoo⁴⁸, S. Sahoo⁶¹, P.K. Sahu⁶¹, J. Saini¹³², S. Sakai⁷⁴, M.A. Saleh¹³⁴, J. Salzwedel²⁰, S. Sambyal⁹¹, V. Samsonov⁸⁶, L. Šándor⁵⁹, A. Sandoval⁶⁴, M. Sano¹²⁸, D. Sarkar¹³², N. Sarkar¹³², P. Sarma⁴⁴, E. Scapparone¹⁰⁴, F. Scarlassara²⁹, C. Schiaua⁷⁸, R. Schicker⁹⁴, C. Schmidt⁹⁷, H.R. Schmidt³⁴, S. Schuchmann⁵³, J. Schukraft³⁵, M. Schulc³⁹, Y. Schutz^{35,113}, K. Schwarz⁹⁷, K. Schweda⁹⁷, G. Scioli²⁷, E. Scomparin¹¹⁰, R. Scott¹²⁵, M. Šefčík⁴⁰, J.E. Seger⁸⁷, Y. Sekiguchi¹²⁷, D. Sekihata⁴⁶, I. Selyuzhenkov⁹⁷, K. Senosi⁶⁵, S. Senyukov^{3,35}, E. Serradilla^{10,64}, A. Sevcenco⁶², A. Shabanov⁵⁶, A. Shabetai¹¹³, O. Shadura³, R. Shahoyan³⁵, M.I. Shahzad¹⁶, A. Shangaraev¹¹¹, A. Sharma⁹¹, M. Sharma⁹¹, M. Sharma⁹¹, N. Sharma¹²⁵, A.I. Sheikh¹³², K. Shigaki⁴⁶, Q. Shou⁷, K. Shtejer^{26,9}, Y. Sibiriak⁸⁰, S. Siddhanta¹⁰⁵, K.M. Sielewicz³⁵, T. Siemiarczuk⁷⁷, D. Silvermyr³³, C. Silvestre⁷¹, G. Simatovic¹²⁹, G. Simonetti³⁵, R. Singaraju¹³², R. Singh⁷⁹, S. Singha^{132,79}, V. Singhal¹³², B.C. Sinha¹³², T. Sinha¹⁰⁰, B. Sitar³⁸, M. Sitta³¹, T.B. Skaali²², M. Slupecki¹²³, N. Smirnov¹³⁶, R.J.M. Snellings⁵⁷, T.W. Snellman¹²³, J. Song⁹⁶, M. Song¹³⁷, Z. Song⁷, F. Soramel²⁹, S. Sorensen¹²⁵, R.D.de Souza¹²¹, F. Sozzi⁹⁷, M. Spacek³⁹, E. Spiriti⁷², I. Sputowska¹¹⁷, M. Spyropoulou-Stassinaki⁸⁹, J. Stachel⁹⁴, I. Stan⁶², P. Stankus⁸⁵, E. Stenlund³³, G. Steyn⁶⁵, J.H. Stiller⁹⁴, D. Stocco¹¹³, P. Strmen³⁸, A.A.P. Suaide¹²⁰, T. Sugitate⁴⁶, C. Suire⁵¹, M. Suleymanov¹⁶, M. Suljic^{25,i}, R. Sultanov⁵⁸, M. Šumbera⁸⁴, S. Sumowidagdo⁴⁹, A. Szabo³⁸, A. Szanto de Toledo^{120,i}, I. Szarka³⁸, A. Szczepankiewicz³⁵, M. Szymanski¹³³, U. Tabassam¹⁶, J. Takahashi¹²¹, G.J. Tambave¹⁸, N. Tanaka¹²⁸, M. Tarhini⁵¹, M. Tariq¹⁹, M.G. Tarzila⁷⁸, A. Tauro³⁵, G. Tejada Muñoz², A. Telesca³⁵, K. Terasaki¹²⁷, C. Terrevoli²⁹, B. Teyssier¹³⁰, J. Thäder⁷⁴, D. Thakur⁴⁸, D. Thomas¹¹⁸, R. Tieulent¹³⁰, A.R. Timmins¹²², A. Toia⁵³, S. Trogolo²⁶, G. Trombetta³², V. Trubnikov³, W.H. Trzaska¹²³, T. Tsuji¹²⁷, A. Tumkin⁹⁹, R. Turrisi¹⁰⁷, T.S. Tveter²², K. Ullaland¹⁸, A. Uras¹³⁰, G.L. Usai²⁴, A. Utrobicic¹²⁹, M. Vala⁵⁹, L. Valencia Palomo⁷⁰, S. Vallero²⁶, J. Van Der Maarel⁵⁷, J.W. Van Hoorne³⁵, M. van Leeuwen⁵⁷, T. Vanat⁸⁴, P. Vande Vyvre³⁵, D. Varga¹³⁵, A. Vargas², M. Vargyas¹²³, R. Varma⁴⁷, M. Vasileiou⁸⁹, A. Vasiliev⁸⁰, A. Vauthier⁷¹, V. Vechemin¹³¹, A.M. Veen⁵⁷, M. Veldhoen⁵⁷, A. Velure¹⁸, E. Vercellin²⁶, S. Vergara Limón², R. Vernet⁸, M. Verweij¹³⁴, L. Vickovic¹¹⁶, G. Viesti^{29,i}, J. Viinikainen¹²³, Z. Vilakazi¹²⁶, O. Villalobos Baillie¹⁰¹, A. Villatoro Tello², A. Vinogradov⁸⁰, L. Vinogradov¹³¹, Y. Vinogradov^{99,i}, T. Virgili³⁰, V. Vislavicius³³, Y.P. Viyogi¹³², A. Vodopyanov⁶⁶, M.A. Völkl⁹⁴, K. Voloshin⁵⁸, S.A. Voloshin¹³⁴, G. Volpe^{32,135}, B. von Haller³⁵, I. Vorobyev^{36,93}, D. Vranic^{97,35}, J. Vrláková⁴⁰, B. Vulpescu⁷⁰, B. Wagner¹⁸, J. Wagner⁹⁷, H. Wang⁵⁷, M. Wang^{7,113}, D. Watanabe¹²⁸, Y. Watanabe¹²⁷, M. Weber^{35,112}, S.G. Weber⁹⁷, D.F. Weiser⁹⁴, J.P. Wessels⁵⁴, U. Westerhoff⁵⁴, A.M. Whitehead⁹⁰, J. Wiechula³⁴, J. Wikne²², G. Wilk⁷⁷, J. Wilkinson⁹⁴, M.C.S. Williams¹⁰⁴, B. Windelband⁹⁴, M. Winn⁹⁴, H. Yang⁵⁷, P. Yang⁷, S. Yano⁴⁶, Z. Yasin¹⁶, Z. Yin⁷, H. Yokoyama¹²⁸, I.-K. Yoo⁹⁶, J.H. Yoon⁵⁰, V. Yurchenko³, I. Yushmanov⁸⁰, A. Zaborowska¹³³, V. Zaccolo⁸¹, A. Zaman¹⁶, C. Zampolli^{104,35}, H.J.C. Zanoli¹²⁰, S. Zaporozhets⁶⁶, N. Zardoshti¹⁰¹, A. Zarochentsev¹³¹, P. Závada⁶⁰, N. Zaviyalov⁹⁹, H. Zbroszczyk¹³³, I.S. Zgura⁶², M. Zhalov⁸⁶, H. Zhang¹⁸, X. Zhang^{74,7}, Y. Zhang⁷, C. Zhang⁵⁷, Z. Zhang⁷, C. Zhao²², N. Zhigareva⁵⁸, D. Zhou⁷, Y. Zhou⁸¹, Z. Zhou¹⁸, H. Zhu¹⁸, J. Zhu^{7,113}, A. Zichichi^{27,12}, A. Zimmermann⁹⁴, M.B. Zimmermann^{54,35}, G. Zinovjev³, M. Zyzak⁴²

Affiliation notes

ⁱ Deceased

ⁱⁱ Also at: Georgia State University, Atlanta, Georgia, United States

ⁱⁱⁱ Also at: Also at Department of Applied Physics, Aligarh Muslim University, Aligarh, India

^{iv} Also at: M.V. Lomonosov Moscow State University, D.V. Skobeltsyn Institute of Nuclear, Physics, Moscow, Russia

Collaboration Institutes

- ¹ A.I. Alikhanyan National Science Laboratory (Yerevan Physics Institute) Foundation, Yerevan, Armenia
- ² Benemérita Universidad Autónoma de Puebla, Puebla, Mexico
- ³ Bogolyubov Institute for Theoretical Physics, Kiev, Ukraine
- ⁴ Bose Institute, Department of Physics and Centre for Astroparticle Physics and Space Science (CAPSS), Kolkata, India
- ⁵ Budker Institute for Nuclear Physics, Novosibirsk, Russia
- ⁶ California Polytechnic State University, San Luis Obispo, California, United States
- ⁷ Central China Normal University, Wuhan, China
- ⁸ Centre de Calcul de l'IN2P3, Villeurbanne, France

- ⁹ Centro de Aplicaciones Tecnológicas y Desarrollo Nuclear (CEADEN), Havana, Cuba
- ¹⁰ Centro de Investigaciones Energéticas Medioambientales y Tecnológicas (CIEMAT), Madrid, Spain
- ¹¹ Centro de Investigación y de Estudios Avanzados (CINVESTAV), Mexico City and Mérida, Mexico
- ¹² Centro Fermi - Museo Storico della Fisica e Centro Studi e Ricerche “Enrico Fermi”, Rome, Italy
- ¹³ Chicago State University, Chicago, Illinois, USA
- ¹⁴ China Institute of Atomic Energy, Beijing, China
- ¹⁵ Commissariat à l’Energie Atomique, IRFU, Saclay, France
- ¹⁶ COMSATS Institute of Information Technology (CIIT), Islamabad, Pakistan
- ¹⁷ Departamento de Física de Partículas and IGFAE, Universidad de Santiago de Compostela, Santiago de Compostela, Spain
- ¹⁸ Department of Physics and Technology, University of Bergen, Bergen, Norway
- ¹⁹ Department of Physics, Aligarh Muslim University, Aligarh, India
- ²⁰ Department of Physics, Ohio State University, Columbus, Ohio, United States
- ²¹ Department of Physics, Sejong University, Seoul, South Korea
- ²² Department of Physics, University of Oslo, Oslo, Norway
- ²³ Dipartimento di Fisica dell’Università ‘La Sapienza’ and Sezione INFN Rome, Italy
- ²⁴ Dipartimento di Fisica dell’Università and Sezione INFN, Cagliari, Italy
- ²⁵ Dipartimento di Fisica dell’Università and Sezione INFN, Trieste, Italy
- ²⁶ Dipartimento di Fisica dell’Università and Sezione INFN, Turin, Italy
- ²⁷ Dipartimento di Fisica e Astronomia dell’Università and Sezione INFN, Bologna, Italy
- ²⁸ Dipartimento di Fisica e Astronomia dell’Università and Sezione INFN, Catania, Italy
- ²⁹ Dipartimento di Fisica e Astronomia dell’Università and Sezione INFN, Padova, Italy
- ³⁰ Dipartimento di Fisica ‘E.R. Caianiello’ dell’Università and Gruppo Collegato INFN, Salerno, Italy
- ³¹ Dipartimento di Scienze e Innovazione Tecnologica dell’Università del Piemonte Orientale and Gruppo Collegato INFN, Alessandria, Italy
- ³² Dipartimento Interateneo di Fisica ‘M. Merlin’ and Sezione INFN, Bari, Italy
- ³³ Division of Experimental High Energy Physics, University of Lund, Lund, Sweden
- ³⁴ Eberhard Karls Universität Tübingen, Tübingen, Germany
- ³⁵ European Organization for Nuclear Research (CERN), Geneva, Switzerland
- ³⁶ Excellence Cluster Universe, Technische Universität München, Munich, Germany
- ³⁷ Faculty of Engineering, Bergen University College, Bergen, Norway
- ³⁸ Faculty of Mathematics, Physics and Informatics, Comenius University, Bratislava, Slovakia
- ³⁹ Faculty of Nuclear Sciences and Physical Engineering, Czech Technical University in Prague, Prague, Czech Republic
- ⁴⁰ Faculty of Science, P.J. Šafárik University, Košice, Slovakia
- ⁴¹ Faculty of Technology, Buskerud and Vestfold University College, Vestfold, Norway
- ⁴² Frankfurt Institute for Advanced Studies, Johann Wolfgang Goethe-Universität Frankfurt, Frankfurt, Germany
- ⁴³ Gangneung-Wonju National University, Gangneung, South Korea
- ⁴⁴ Gauhati University, Department of Physics, Guwahati, India
- ⁴⁵ Helsinki Institute of Physics (HIP), Helsinki, Finland
- ⁴⁶ Hiroshima University, Hiroshima, Japan
- ⁴⁷ Indian Institute of Technology Bombay (IIT), Mumbai, India
- ⁴⁸ Indian Institute of Technology Indore, Indore (IITI), India
- ⁴⁹ Indonesian Institute of Sciences, Jakarta, Indonesia
- ⁵⁰ Inha University, Incheon, South Korea
- ⁵¹ Institut de Physique Nucléaire d’Orsay (IPNO), Université Paris-Sud, CNRS-IN2P3, Orsay, France
- ⁵² Institut für Informatik, Johann Wolfgang Goethe-Universität Frankfurt, Frankfurt, Germany
- ⁵³ Institut für Kernphysik, Johann Wolfgang Goethe-Universität Frankfurt, Frankfurt, Germany
- ⁵⁴ Institut für Kernphysik, Westfälische Wilhelms-Universität Münster, Münster, Germany
- ⁵⁵ Institut Pluridisciplinaire Hubert Curien (IPHC), Université de Strasbourg, CNRS-IN2P3, Strasbourg, France
- ⁵⁶ Institute for Nuclear Research, Academy of Sciences, Moscow, Russia
- ⁵⁷ Institute for Subatomic Physics of Utrecht University, Utrecht, Netherlands
- ⁵⁸ Institute for Theoretical and Experimental Physics, Moscow, Russia
- ⁵⁹ Institute of Experimental Physics, Slovak Academy of Sciences, Košice, Slovakia

- 60 Institute of Physics, Academy of Sciences of the Czech Republic, Prague, Czech Republic
- 61 Institute of Physics, Bhubaneswar, India
- 62 Institute of Space Science (ISS), Bucharest, Romania
- 63 Instituto de Ciencias Nucleares, Universidad Nacional Autónoma de México, Mexico City, Mexico
- 64 Instituto de Física, Universidad Nacional Autónoma de México, Mexico City, Mexico
- 65 iThemba LABS, National Research Foundation, Somerset West, South Africa
- 66 Joint Institute for Nuclear Research (JINR), Dubna, Russia
- 67 Konkuk University, Seoul, South Korea
- 68 Korea Institute of Science and Technology Information, Daejeon, South Korea
- 69 KTO Karatay University, Konya, Turkey
- 70 Laboratoire de Physique Corpusculaire (LPC), Clermont Université, Université Blaise Pascal, CNRS-IN2P3, Clermont-Ferrand, France
- 71 Laboratoire de Physique Subatomique et de Cosmologie, Université Grenoble-Alpes, CNRS-IN2P3, Grenoble, France
- 72 Laboratori Nazionali di Frascati, INFN, Frascati, Italy
- 73 Laboratori Nazionali di Legnaro, INFN, Legnaro, Italy
- 74 Lawrence Berkeley National Laboratory, Berkeley, California, United States
- 75 Moscow Engineering Physics Institute, Moscow, Russia
- 76 Nagasaki Institute of Applied Science, Nagasaki, Japan
- 77 National Centre for Nuclear Studies, Warsaw, Poland
- 78 National Institute for Physics and Nuclear Engineering, Bucharest, Romania
- 79 National Institute of Science Education and Research, Bhubaneswar, India
- 80 National Research Centre Kurchatov Institute, Moscow, Russia
- 81 Niels Bohr Institute, University of Copenhagen, Copenhagen, Denmark
- 82 Nikhef, Nationaal instituut voor subatomaire fysica, Amsterdam, Netherlands
- 83 Nuclear Physics Group, STFC Daresbury Laboratory, Daresbury, United Kingdom
- 84 Nuclear Physics Institute, Academy of Sciences of the Czech Republic, Řež u Prahy, Czech Republic
- 85 Oak Ridge National Laboratory, Oak Ridge, Tennessee, United States
- 86 Petersburg Nuclear Physics Institute, Gatchina, Russia
- 87 Physics Department, Creighton University, Omaha, Nebraska, United States
- 88 Physics Department, Panjab University, Chandigarh, India
- 89 Physics Department, University of Athens, Athens, Greece
- 90 Physics Department, University of Cape Town, Cape Town, South Africa
- 91 Physics Department, University of Jammu, Jammu, India
- 92 Physics Department, University of Rajasthan, Jaipur, India
- 93 Physik Department, Technische Universität München, Munich, Germany
- 94 Physikalisches Institut, Ruprecht-Karls-Universität Heidelberg, Heidelberg, Germany
- 95 Purdue University, West Lafayette, Indiana, United States
- 96 Pusan National University, Pusan, South Korea
- 97 Research Division and ExtreMe Matter Institute EMMI, GSI Helmholtzzentrum für Schwerionenforschung, Darmstadt, Germany
- 98 Rudjer Bošković Institute, Zagreb, Croatia
- 99 Russian Federal Nuclear Center (VNIIEF), Sarov, Russia
- 100 Saha Institute of Nuclear Physics, Kolkata, India
- 101 School of Physics and Astronomy, University of Birmingham, Birmingham, United Kingdom
- 102 Sección Física, Departamento de Ciencias, Pontificia Universidad Católica del Perú, Lima, Peru
- 103 Sezione INFN, Bari, Italy
- 104 Sezione INFN, Bologna, Italy
- 105 Sezione INFN, Cagliari, Italy
- 106 Sezione INFN, Catania, Italy
- 107 Sezione INFN, Padova, Italy
- 108 Sezione INFN, Rome, Italy
- 109 Sezione INFN, Trieste, Italy
- 110 Sezione INFN, Turin, Italy
- 111 SSC IHEP of NRC Kurchatov institute, Protvino, Russia
- 112 Stefan Meyer Institut für Subatomare Physik (SMI), Vienna, Austria

- 113 SUBATECH, Ecole des Mines de Nantes, Université de Nantes, CNRS-IN2P3, Nantes, France
- 114 Suranaree University of Technology, Nakhon Ratchasima, Thailand
- 115 Technical University of Košice, Košice, Slovakia
- 116 Technical University of Split FESB, Split, Croatia
- 117 The Henryk Niewodniczanski Institute of Nuclear Physics, Polish Academy of Sciences, Cracow, Poland
- 118 The University of Texas at Austin, Physics Department, Austin, Texas, USA
- 119 Universidad Autónoma de Sinaloa, Culiacán, Mexico
- 120 Universidade de São Paulo (USP), São Paulo, Brazil
- 121 Universidade Estadual de Campinas (UNICAMP), Campinas, Brazil
- 122 University of Houston, Houston, Texas, United States
- 123 University of Jyväskylä, Jyväskylä, Finland
- 124 University of Liverpool, Liverpool, United Kingdom
- 125 University of Tennessee, Knoxville, Tennessee, United States
- 126 University of the Witwatersrand, Johannesburg, South Africa
- 127 University of Tokyo, Tokyo, Japan
- 128 University of Tsukuba, Tsukuba, Japan
- 129 University of Zagreb, Zagreb, Croatia
- 130 Université de Lyon, Université Lyon 1, CNRS-IN2P3, IPN-Lyon, Villeurbanne, France
- 131 V. Fock Institute for Physics, St. Petersburg State University, St. Petersburg, Russia
- 132 Variable Energy Cyclotron Centre, Kolkata, India
- 133 Warsaw University of Technology, Warsaw, Poland
- 134 Wayne State University, Detroit, Michigan, United States
- 135 Wigner Research Centre for Physics, Hungarian Academy of Sciences, Budapest, Hungary
- 136 Yale University, New Haven, Connecticut, United States
- 137 Yonsei University, Seoul, South Korea
- 138 Zentrum für Technologietransfer und Telekommunikation (ZTT), Fachhochschule Worms, Worms, Germany